ACS APPLIED MATERIALS & INTERFACES

Research Article

www.acsami.org

Novel Peptide-Based Platform for the Dual Presentation of Biologically Active Peptide Motifs on Biomaterials

Carlos Mas-Moruno,*[,†,‡,§] Roberta Fraioli,[†,‡,§] Fernando Albericio,[‡,⊥,#,∥] José María Manero,[†,‡] and F. Javier Gil[†,‡]

[†]Biomaterials, Biomechanics and Tissue Engineering Group, Department of Materials Science and Metallurgical Engineering, Technical University of Catalonia (UPC), ETSEIB, Avenida Diagonal 647, 08028 Barcelona, Spain

[‡]Biomedical Research Networking Centre in Bioengineering, Biomaterials and Nanomedicine (CIBER-BBN), Campus Río Ebro, Edificio I+D Bloque 5, 1a planta, C/Poeta Mariano Esquillor s/n, 50018 Zaragoza, Spain

[§]Centre for Research in NanoEngineering (CRNE), Universitat Politécnica de Catalunya, C/Pascual i Vila 15, 08028 Barcelona, Spain

[⊥]Institute for Research in Biomedicine (IRB-Barcelona), Barcelona Science Park, C/Baldiri Reixac 10, 08028 Barcelona, Spain

[#]Department of Organic Chemistry, University of Barcelona, C/Martí i Franquès 1-11, 08028 Barcelona, Spain

[∥]School of Chemistry & Physics, University of KwaZulu-Natal, 4001 Durban, South Africa

Supporting Information

ABSTRACT: Biofunctionalization of metallic materials with cell adhesive molecules derived from the extracellular matrix is a feasible approach to improve cell−material interactions and enhance the biointegration of implant materials (e.g., osseointegration of bone implants). However, classical biomimetic strategies may prove insufficient to elicit complex and multiple biological signals required in the processes of tissue regeneration. Thus, newer strategies are focusing on installing multifunctionality on biomaterials. In this work, we introduce a novel peptide-based divalent platform with the capacity to simultaneously present distinct bioactive peptide motifs in a chemically controlled fashion. As a proof of concept, the integrin-binding sequences RGD and PHSRN were selected and introduced in the platform. The biofunctionalization of titanium with this platform showed a positive trend towards increased numbers of cell attachment, and statistically higher values of spreading and proliferation of osteoblast-like cells compared to control noncoated samples. Moreover, it displayed statistically comparable or improved cell responses compared to samples coated with the single peptides or with an equimolar mixture of the two motifs. Osteoblast-like cells produced higher levels of alkaline phosphatase on surfaces functionalized with the platform than on control titanium; however, these values were not statistically significant. This study demonstrates that these peptidic structures are versatile tools to convey multiple biofunctionality to biomaterials in a chemically defined manner.

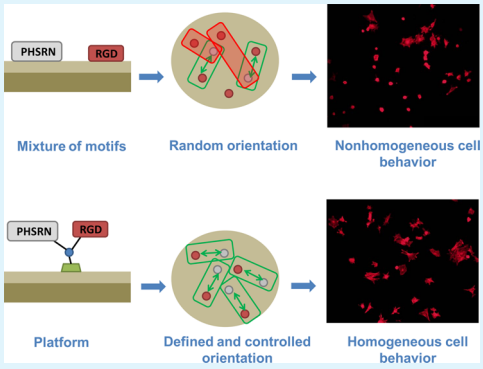

KEYWORDS: *biofunctionalization, cell adhesive peptide, cell adhesion, peptide platform, titanium, RGD peptide, PHSRN peptide*

INTRODUCTION

It is nowadays well-established that the biofunctionalization of metallic materials with cell adhesive molecules derived from the extracellular matrix (ECM) is a powerful approach to stimulate and direct cell behavior (i.e., cell adhesion, proliferation and differentiation), and thus improve and accelerate the biointegration of an implant material within the organism.[1−3] Such biomimetic strategy relies on the interaction of short cell binding peptide sequences of the ECM with cell-expressed receptors such as integrins, which trigger intracellular biochemical signals and mediate specific cellular functions.[4] In regard to this, the functionalization of Ti surfaces with proteins or peptides with affinity for integrins expressed by osteoblasts has shown to enhance osteoblast adhesion to these surfaces in vitro and improve implant osseointegration in vivo.[1,5,6]

Nonetheless, there is a long-standing debate concerning which is the best biomimetic approach to convey functionality to biomaterials.[7] The use of native proteins (e.g., fibronectin,[8,9] type I collagen[10−12]) or recombinant protein fragments (e.g. FNIII-(7−10),[13−15] FNIII(9−10)[16]) from the ECM provides multiple and dynamic bioactive epitopes that efficiently engage and activate complex cellular responses. Nonetheless, this approach presents some limitations related to the low stability of proteins towards changes of pH and temperature, the risks of infection and immunogenicity associated with their use, the difficulty in obtaining chemically defined structures, and their high costs of production.[17,18]

Received: January 7, 2014
Accepted: March 27, 2014
Published: March 27, 2014

   dx.doi.org/10.1021/am5001213 | ACS Appl. Mater. Interfaces 2014, 6, 6525−6536

Using short synthetic peptides, encompassing only the amino acids required to promote cell adhesion events like the tripeptide sequence Arg-Gly-Asp (RGD),[19,20] may overcome most limitations associated with the use of proteins. However, single peptide motifs often fail to recapitulate the full biological potential of a protein and display poor selectivity profiles.[1,5,6,17,18,21] In this regard, great effort has been devoted to improve the biological activity and selectivity of cell adhesive peptides through design of cyclic peptides and peptidomimetics.[5,6,22] Such approaches have yielded surfaces with enhanced affinities for integrin subtypes $\alpha v\beta 3$ and $\alpha v\beta 5$ (and selective against the platelet receptor $\alpha IIb\beta 3$),[23,24] or even with the capability to discriminate between $\alpha v\beta 3$ and $\alpha 5\beta 1$.[25−27] Yet, as promising as these approaches may be, it is unlikely that these molecules will be able to emulate the intricate nature of cell-ECM interactions that are necessary for complex cellular responses.

A simple, though useful approach to install multifunctionality on surfaces while taking advantage of the optimal properties offered by short synthetic peptides is to combine distinct bioactive sequences having multiple, either complementary or synergistic, biological effects. For example, the combination of the integrin-binding RGD motif with heparin-binding sequences such as FHRRIKA or KRSR[28,29] has shown to enhance osteoblast-like cell attachment and mineralization compared to the use of the single peptides.[30−32] Another well-documented example is the use of the RGD sequence together with the PHSRN motif, a sequence that was found in fibronectin to synergize its RGD-mediated binding to $\alpha 5\beta 1$.[33] These two synthetic sequences have been combined either as mixtures[34−37] or in linear oligopeptides[38−41] and peptide amphiphiles,[35] and their immobilization onto surfaces displayed improved cell adhesive events in comparison with the RGD sequence alone. The main limitation of this strategy is that it is difficult to reproduce the expected spacing and orientation of the ligands, and that the characterization of the exact ratio of molecules bound to the surface is not trivial.

On the basis of these premises, the aim of our work was to introduce a versatile and easy-to-synthesize peptide-based platform to functionalize biomaterials, and simultaneously present two distinct biologically-active peptide motifs in a chemically controlled and defined fashion. This system contains the following functional features, which are schematically depicted in Figure 1:

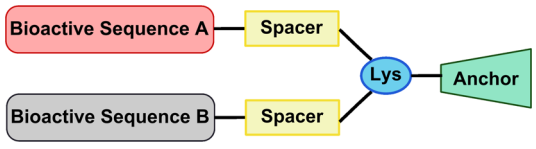

Figure 1. Schematic representation of the peptide-based divalent platform, consisting of (i) two distinct bioactive peptide sequences, (ii) two spacer moieties, (iii) a lysine (Lys) residue as branching unit, and (iv) an anchoring group.

(i) Two bioactive sequences, which may be combined from a wide range of biologically-relevant peptide motifs to exert different biofunctionalities simultaneously: enhanced and/or selective cell adhesion, activation of synergistic domains, specific stimulation of stem cell differentiation, anti-fouling and/or anti-bacterial properties, etc;
(ii) Spacer units to fine-tune the optimal spacing and orientation of the active sequences, and ensure their correct presentation and accessibility;
(iii) An orthogonally-protected lysine (Lys), which serves as branching unit in the construction of the divalent architecture;
(iv) And an anchoring group to provide a chemoselective, strong and stable binding of the molecule to the material.

Here, as a proof of concept study, the well known cell adhesive RGD[19] and PHSRN[33] sequences were selected and introduced in the peptide-based platform. To determine the feasibility of this new strategy, the divalent platform was synthesized, immobilized onto Ti samples, and the response of sarcoma osteogenic (Saos-2) cells to these surfaces evaluated in vitro by means of cell adhesion, proliferation, and differentiation assays. The effect of the dual co-presentation of RGD and PHSRN motifs in the platform was compared with the immobilization of the single peptide motifs either alone or as a mixture.

MATERIALS AND METHODS

Ti Biofunctionalization. *General: Chemicals and Instrumentation.* Commercially pure (c.p.) grade 2 Ti bars were obtained from Technalloy S.A. (Sant Cugat del Vallès, Spain) and silicon carbide (SiC) grinding papers from Neuertek S.A. (Eibar, Spain) and Beortek S.A. (Asua-Erandio, Spain). Fmoc-Rink amide MBHA resin, 2-chlorotrityl chloride (CTC) resin and Fmoc-L-amino acids were purchased from Iris Biotech GmbH (Marktredwitz, Germany). Coupling reagents were obtained from Sigma-Aldrich (St Louis, MO, USA), Medalchemy (Alicante, Spain), Luxembourg Industries Ltd. (Tel Aviv, Israel) and Alfa Aesar (Karlsruhe, Germany). All other chemicals and solvents were acquired from Sigma-Aldrich, Alfa Aesar and SDS (Peypin, France). Analytical high-performance liquid chromatography (HPLC) was performed using a Waters Alliance 2695 chromatography system (Waters, Milford, MA, USA), a reversed-phase XBridge BEH130 C-18 column (4.6 mm × 100 mm, 3.5 μm) and a photodiode array detector (Waters 2998). The system was run at a flow rate of 1.0 mL/min over 8 min at room temperature using water (0.045 % trifluoroacetic acid (TFA), v/v) and acetonitrile (ACN) (0.036 % TFA, v/v) as solvents. Semi-preparative HPLC purification was conducted on a Waters Delta 600 instrument with a dual λ absorbance detector (Waters 2487) using a reversed-phase Sunfire OBD C-18 column (19 mm × 100 mm, 5.0 μm) at a flow rate of 15 mL/min for 12 min. Mass spectra were recorded on a MALDI-TOF Voyager DE RP spectrometer (Applied Biosystems, Foster City, CA, USA).

Preparation of Ti Disks. Ti disks (2 mm thick, 10 mm diameter) were obtained from c.p. grade 2 Ti bars. Mirror-like, smooth surfaces ($R_a \leq$ 40 nm) were achieved by grinding with SiC papers of decreasing grit size (from P800 to P2400 − European P-grade standard), followed by polishing with suspensions of alumina particles (1 μm and 0.05 μm particle size) on cotton clothes. Prior to functionalization, samples were ultrasonically rinsed with cyclohexane, isopropanol, distilled water, ethanol and acetone. Samples were stored dry under vacuum.

Solid-Phase Peptide Synthesis (SPPS). Synthesis of Linear Control Peptides (RGD and PHSRN). The linear peptides MPA-Ahx-Ahx-Ahx-Arg-Gly-Asp-Ser-OH (RGD) and MPA-Ahx-Ahx-Ahx-Pro-His-Ser-Arg-Asn-NH_2 (PHSRN) (Ahx: aminohexanoic acid; MPA: 3-mercaptopropionic acid) were manually synthesized by SPPS methods following the Fmoc/tBu strategy and using CTC resin (200 mg, 1.0 mmol/g) or Fmoc-Rink amide MBHA resin (200 mg, 0.45 mmol/g), respectively, as solid supports. The Fmoc group was removed by treatment with piperidine/*N*,*N*-dimethylformamide (DMF) (20:80, v/v) and coupling reactions were carried out with Fmoc-L-amino acids (4 equiv), ethyl 2-cyano-2-(hydroxyimino)acetate (OxymaPure) (4 equiv), and *N*,*N*′-diisopropylcarbodiimide (DIC) (4 equiv) in DMF for 45 min at room temperature. Alternatively, the coupling of sterically more demanding amino acids was performed using N-[(dimethylamino)-1H-1,2,3-triazolo[4,5-*b*]pyridino-1-ylmethylene]-*N*-methylmethanaminium hexafluorophosphate (HATU) (4 equiv) and *N*,*N*-diisopropylethylamine (DIEA) (8 equiv) as coupling system. The efficiency of each reaction was monitored using the Kaiser test and by analytical HPLC analysis. After completion of the synthesis, peptides were cleaved from

dx.doi.org/10.1021/am5001213 | ACS Appl. Mater. Interfaces 2014, 6, 6525−6536

the solid support with concomitant deprotection of the side chain protecting groups. To this end, the resin was washed with dichloromethane (DCM), dried, and treated with TFA/water/triisopropylsilane (TIS) (85:10:5, v/v/v) for 1.5 h in the presence of small amounts of dithiothreitol (DTT) to prevent from thiol oxidation. Peptides were then precipitated with cold diethyl ether, centrifuged and washed twice with diethyl ether. The crude peptides were finally dissolved in water/ACN (1:1, v/v) and lyophilized. Purification of the peptides was achieved by semi-preparative HPLC using linear gradients from 10 to 40 % ACN over 12 min (RGD) and 0 to 40 % ACN over 12 min (PHSRN). The purified peptides were characterized by analytical HPLC and MALDI-TOF. RGD: HPLC (10 to 40 % ACN over 8 min, t_R = 4.345 min, purity >99 %), MALDI-TOF (m/z calcd for $C_{36}H_{64}N_{10}O_{12}S$, 860.44; found, 861.78 [M + H]+); PHSRN: HPLC (0 to 45 % ACN over 8 min, t_R = 6.115 min, purity >99 % MALDI-TOF (m/z calcd for $C_{45}H_{77}N_{15}O_{11}S$, 1035.56; found, 1037.01 [M + H]+).

Synthesis of the Dimeric Platform. The dimeric platform (Ac-Arg-Gly-Asp-Ser-Ahx-Ahx)(Ac-Pro-His-Ser-Arg-Asn-Ahx-Ahx)-Lys-βAla-Cys-NH_2 was manually synthesized on Fmoc-Rink amide MBHA resin (200 mg, 0.45 mmol/g) following the SPPS protocols described for the synthesis of the linear peptides (Figure 2). The synthesis started with the attachment of Fmoc-Cys(Trt)-OH to the resin, followed by the coupling of Fmoc-βAla-OH as spacing unit. Next, the introduction of Fmoc-Lys(Alloc)-OH and selective deprotection of the α-amino Fmoc protecting group by piperidine treatment allowed the elongation of the first branch of the platform (the RGD sequence). The N-terminus of this peptide sequence was acetylated after treatment with Ac_2O/DIEA/DMF (10:20:70, v/v/v) (1 × 5 min, 2 × 10 min). To construct the second active motif (the PHSRN sequence), the Alloc group was

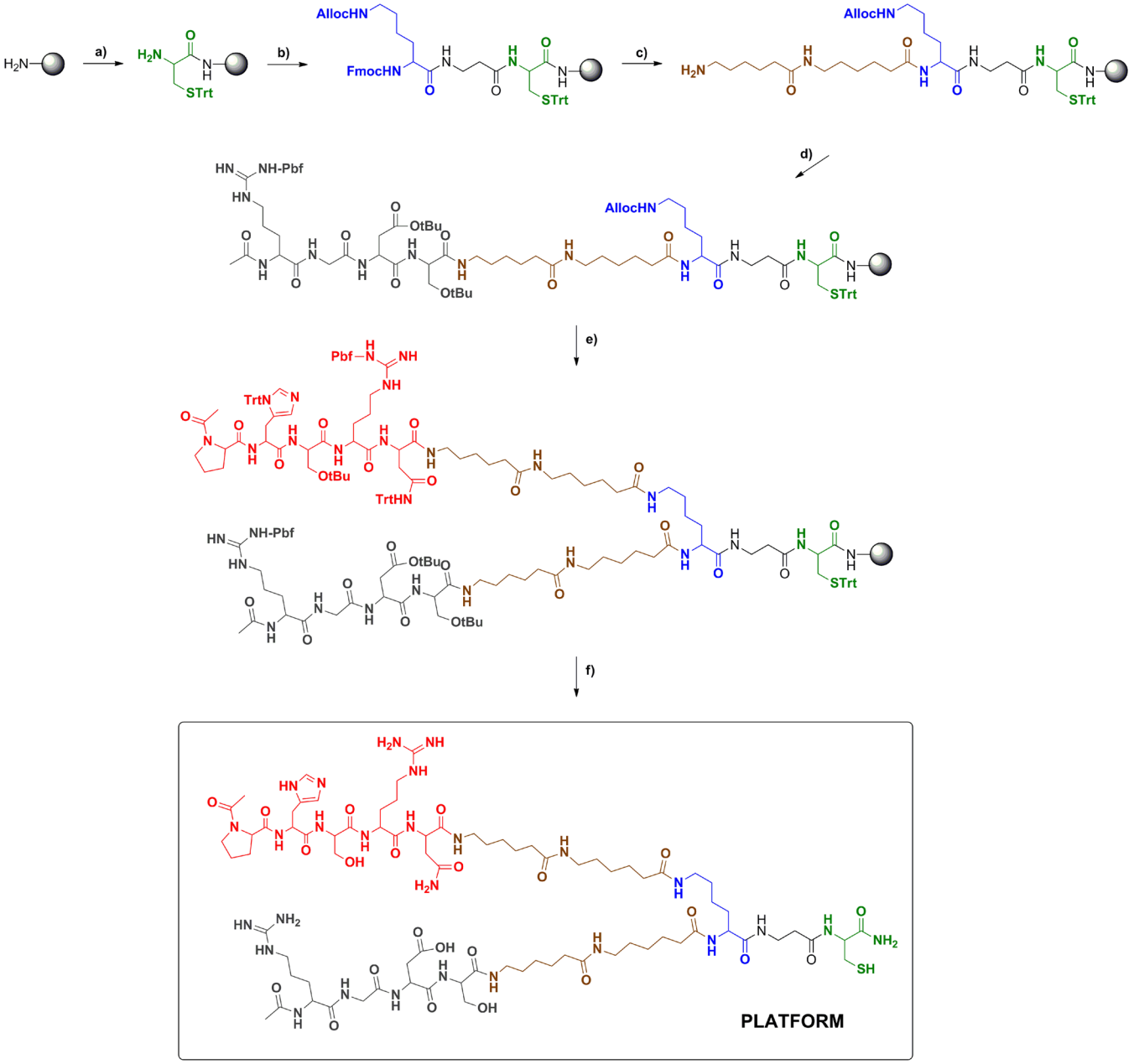

Figure 2. Solid-phase peptide synthesis (SPPS) of the divalent platform. (a) Coupling of Cys (green) to Rink Amide MBHA resin. (b) Introduction of the Lys branching unit (blue). (c) Selective deprotection of the α-amino and introduction of the spacer (brown). (d) Elongation of the RGDS motif (grey). (e) Elongation of the second branch (spacer and PHSRN motif (red)). (f) Side-chain deprotection and cleavage from the resin (the complete SPPS experimental protocols are described in the main text).

dx.doi.org/10.1021/am5001213 | ACS Appl. Mater. Interfaces 2014, 6, 6525−6536

removed after 3 × 15 min treatments of $PhSiH_3$ (10 equiv) and $Pd(PPh_3)_4$ (0.1 equiv) in DCM. The resin was then washed with sodium dithiodiethylcarbamate (0.02 M in DMF, 3 × 15 min) to remove any remaining palladium traces off the resin. The N-terminus of this branch was also acetylated as previously described. Finally, the peptide was cleaved from the resin by reaction with TFA/water/TIS (85:10:5, v/v/v) for 3.5 h in the presence of DTT. The work-up of the peptide was performed as explained above and finally purified by means of semi-preparative HPLC (linear gradient from 0 to 40 % ACN over 12 min). The peptidic platform was characterized by analytical HPLC (0 to 40 % ACN over 8 min, t_R = 5.572 min, purity >99 %, Figure S1 in the Supporting Information) and MALDI-TOF (m/z calcd. for $C_{79}H_{135}N_{27}O_{23}S$, 1861.99; found, 1863.71 [M + H]+).

Immobilization of Biomolecules onto Ti Disks. The biomolecules were dissolved in phosphate buffered saline (PBS) at 100 μM and 100 μL of these solutions were deposited onto the Ti samples overnight at room temperature. Control samples were only treated with PBS. Fibronectin was used as positive control in the cellular studies and coated to Ti disks at a concentration of 50 μg/mL in PBS. This concentration of protein was shown to be sufficient to elicit optimal cellular responses on Ti surfaces.[42,43] After peptide immobilization, samples were gently washed with PBS and dried with nitrogen. The biofunctionalized samples, and their controls, are codified as follows:

Ctrol: noncoated Ti

RGD: Ti coated with 100 μM of RGD peptide

PHSRN: Ti coated with 100 μM of PHSRN peptide

MIX: Ti coated with an equimolar mixture of RGD and PHSRN peptides (100 μM each)

Platform: Ti coated with 100 μM of the platform containing the RGD and PHSRN sequences

FN: Ti coated with 50 μg/mL of fibronectin (positive control)

Physicochemical Characterization of the Biofunctionalized Surfaces. *Static Contact Angle Measurements and Surface Energy Calculations.* Static contact angle measurements on Ti surfaces were performed using a contact angle system OCA15 plus (Dataphysics, Filderstadt, Germany) with the sessile drop method. All measurements were done at room temperature using ultrapure Milli-Q water and diiodomethane as wetting liquids (drop volume of 1 μL). Static contact angles were calculated using a Laplace−Young fitting with SCA 20 software (Dataphysics). Contact angle values presented here represent the mean of three measurements per disk for three sample replicates.

The surface energy (SE) and its dispersive and polar components were determined using the Young−Laplace (1) and Owen−Wendt (2) equations.

$$\gamma_S = \gamma_{SL} + \gamma_L \cos\theta \quad (1)$$

$$\gamma_L(1 + \cos\theta) = 2((\gamma_L^d \gamma_S^d)^{1/2} + (\gamma_L^p \gamma_S^p)^{1/2}) \quad (2)$$

Where γ_S is the surface tension of the solid (S), γ_L the surface tension of the liquid (L), γ_{SL} the interfacial free energy or SE between L and S, θ the contact angle between L and S, and γ^d and γ^p represent the dispersive and polar components of the SE, respectively.

Roughness Analysis. The surface roughness of Ti samples was determined using a white light interferometer microscope (Wyko NT9300 Optical Profiler, Veeco Instruments, New York, NY, USA) in vertical scanning interferometry mode. Data analysis was performed with Wyko Vision 4.10 software (Veeco Instruments). Roughness parameters were measured by triplicate for each sample. For each surface treatment three disks were analyzed.

X-ray Photoelectron Spectroscopy (XPS). The chemical composition of the functionalized Ti samples was analyzed using an XPS equipment (SPECS Surface Nano Analysis GmbH, Berlin, Germany) with a Mg anode XR50 source operating at 150 W and a Phoibos 150 MCD-9 detector. High resolution spectra were recorded with a pass energy of 25 eV at 0.1 eV steps at a pressure below 7.5 × 10^{-9} mbar. Binding energies were referred to the C 1s signal at 284.8 eV. For each series three samples were studied. Data was analyzed using CasaXPS software (Version 2.3.16, Casa Software Ltd., Teignmouth, UK).

Biological Characterization of the Biofunctionalized Surfaces. *Cell Culture.* Cellular experiments were conducted using the human osteosarcoma cell line (Saos-2) as osteoblast-like cellular model. Saos-2 cells were cultured in McCoy's 5A medium (Sigma-Aldrich) supplemented with 10% (v/v) fetal bovine serum (FBS), 50 U/mL penicillin, 50 μg/mL streptomycin and 1% (w/v) L-glutamine. Cells were maintained at 37 °C, in a humidified atmosphere containing 5% (v/v) CO_2, changing culture medium twice a week. Upon reaching confluence, cells were detached by trypsin-EDTA and subcultured into a new flask. All experiments were performed using cells at passages between 25 and 35.

Cell Adhesion Studies. To characterize the efficiency of the biofunctionalization of Ti substrates on short-term cell adhesion events, both the number and the spreading of adherent Saos-2 cells was analyzed. To this end, functionalized Ti samples were first transferred into 48-well plates and blocked with 1% (w/v) bovine serum albumin (BSA) in PBS for 30 min at room temperature. This step was done to reduce non-specific interactions between the cells and the surface. Next, Saos-2 cells were seeded at a density of 25 000 cells per disk and allowed to attach in serum free medium. After 4 h of incubation at 37 °C, samples were rinsed twice with PBS to remove non-adherent cells. To determine the number of adherent cells, cells were lysed with 300 μL/disk of mammalian protein extraction reagent (M-PER) and the activity of lactate dehydrogenase (LDH) enzyme was measured by means of a conventional colorimetric assay (Cytotoxicity Detection Kit (LDH), Roche Diagnostics, Mannheim, Germany) using a multimode microplate reader (Infinite M200 PRO, Tecan Group Ltd., Männedorf, Switzerland). To convert the absorbance read-out of the test into cell numbers, a standard curve of defined cell concentrations was applied. Alternatively, staining of nuclei, actin fibers and vinculin was performed to provide additional information on spreading and focal contact formation of adherent cells on the functionalized surfaces. To this end, cells attached to the surfaces were fixed for 30 min with 4% (w/v) paraformaldehyde (PFA). Next, cells were permeabilized with 500 μL/disk of 0.05% (w/v) triton X-100 in PBS for 20 min and blocked with 1 % BSA (w/v) in PBS for 30 min. Washings between steps were all performed with PBS-Gly (PBS containing 20 mM of glycine) for 3 × 5 min. Then, 100 μL/disk of primary antibody mouse anti-vinculin (1:100 in 1 % (w/v) BSA in PBS) were incubated onto the Ti samples for 1 h. The secondary antibody, anti-mouse Alexa 488 (1:2000), and phalloidin-rodhamine (1:300) were both incubated in triton 0.05 % (w/v) in PBS for 1 h in the dark. In a final step, nuclei of cells were also stained with 500 μL/disk of DAPI (1:1000) in PBS-Gly for 2 min in the dark. Metallic disks were then mounted on microscope slides and analyzed by fluorescence microscopy (Nikon E600, Tokyo, Japan). The number and spreading of cells attached on each surfaces was assessed using ImageJ 1.46R software (NIH, Bethesda, MD, USA). Cell numbers were calculated by counting cell nuclei on five fields per disk and measuring the mean values. This analysis was done for three replicates. Spreading of adherent cells was measured for at least 10 cells for each sample and averaged for three samples for each condition. All cellular studies were done using triplicates and repeated at least in two independent assays to ensure reproducibility.

Cell Proliferation. To determine the proliferation of Saos-2 cells on functionalized Ti surfaces, 10 000 cells were seeded on each sample and incubated in serum free medium at 37 °C. After 4 h of incubation, the medium was aspired and replaced by fresh medium supplemented with 10% (v/v) FBS. Medium was then changed twice a week. After 3 and 14 days of incubation, adhering cells were lysed and cell numbers calculated according to the previously described LDH colorimetric assay.

Cell Differentiation. A colorimetric assay (SensoLyte pNPP Alkaline Phosphatase Assay Kit, AnaSpec Inc., Fremont, CA, USA) was used to determine the alkaline phosphatase (ALP) activity by Saos-2 cells, which is known to be an early marker of osteoblastic differentiation. In brief, cells were seeded on functionalized samples as described for the cell proliferation assay and incubated for 14 days. At the end of the incubation period, samples were rinsed twice with PBS, and remaining cells were lysed as indicated above. The activity of ALP was determined by measuring the conversion of p-nitrophenyl phosphate (pNPP) into p-nitrophenol (pNP) according to the manufacturer's instructions.

ALP activity was expressed as nanograms of the enzyme and normalized by the number of cells on each sample.

Statistical Analysis. All data presented in this study are given as mean values ± standard deviations. Significant differences between group means were analyzed by ANOVA test followed by post-hoc pairwise comparisons using Tukey's test, which corrects for experiment-wise error rate. Differences were also analyzed by Kruskal–Wallis non-parametric test followed by Mann-Whitney test, obtaining very similar results. Confidence levels were set at 95% unless otherwise stated.

RESULTS AND DISCUSSION

Design and Synthesis of the Platform. The principal structural features of the platform presented in this study are shown in Figure 1 and classified as four main elements: (i) two distinct bioactive sequences, (ii) spacer units, (iii) a Lys residue, and (iv) an anchoring group.

As previously introduced, the grafting of biomaterials with the combination of RGD and PHSRN cell adhesive sequences has been extensively described to positively influence cell behavior onto these functionalized surfaces. Thus, these two bioactive motifs were excellent candidates to prove the feasibility of our strategy. To ensure that a minimum distance between the active sequences and the material is maintained, and that the two motifs are adequately accessible to interact with cell-expressed integrin receptors, the use of spacer units is required.[26,44] In this particular case, the presentation of the RGD and PHSRN motifs in an optimal conformation is crucial.[38,45,46] The two motifs should ideally be separated 35–40 Å, mimicking the orientation and spacing found in the natural protein fibronectin.[47,48] Different research groups have attempted to mimic this distance by using linkers of different length and chemistry. Although original reports estimated a polyglycine linker of 6 glycine (Gly) units as the optimal spacer length,[38,39,49] further works described longer linkers of 12 Gly[40,50] or 5 serine (Ser)-Gly units[35,51] as more accurate systems. Our design selected 4 aminohexanoic acid (Ahx) units linked via a Lys residue as spacer (Figure 2). Such spacer covers approximately the same distance of 12 Gly, but has enough flexibility to adopt other conformations.[52] The presence of the Lys, in addition to its crucial role in the synthesis (see below), also helps to present these spacer units in a branched configuration, allowing a better accessibility and orientation of the active motifs, compared to that expected for a linear presentation.[21] The design of the platform also had to consider the presence of a suitable anchor to bind the molecule to the implant material (i.e., Ti). To this end, the amino acid cysteine (Cys), which contains a thiol group as side chain functionality, was chosen. Besides the well-characterized affinity that these groups present for gold surfaces and other metals,[25,27,53] thiols have also shown the capacity to bind to titanium oxide (TiO_2).[54] The process of peptide physisorption on TiO_2 is mainly driven by electrostatic interactions, van der Waals forces and/or hydrogen bonds between the amino (NH_3^+) and carboxyl (COO^-) groups of the peptides and the TiO_2 surfaces.[55] According to molecular dynamic studies on the adsorption of several amino acids on rutile (TiO_2), more stable bindings may be attained by the formation of chemical bonds between thiol groups of Cys and Ti atoms of the surface.[54] In this regard, thiols have been used to immobilize RGD-based cyclic peptides and peptidomimetics to Ti surfaces and retained the biological activity of the bioactive molecules both in vitro[24,44] and in vivo.[56,57] This method of immobilization allows a simple, one-step coating of the Ti surface, and it does not require to conduct excessive chemistry on the surface as with other methodologies of functionalization.[31,37] It should be mentioned that phosphonic acids are preferable anchors to bind to Ti because they establish strong and very stable interactions with this metal;[58] however, their use is synthetically more demanding than thiols, which can be easily incorporated as Cys residues.

Once the main elements of the design were established, the peptidic platform was synthesized stepwise in solid-phase as described in Materials and Methods (Figure 2). The orthogonally protected Fmoc-Lys(Alloc)-OH represents the key synthetic component in the preparation of the branched structure due to its scheme of protecting groups. The α-amino Fmoc protecting group is labile to the treatment with bases, and can be easily removed by reaction with piperidine, without affecting the integrity of the ε-amino Alloc group. This strategy, frequently used in the design of cyclic peptides,[59] allows elongating the molecule only at the N-α position. It is important to follow this order of deprotection because the removal of the Alloc group in the first place has been associated with premature and undesired elimination of the Fmoc group.[60] After completion of the synthesis of the first branch, the use of catalytic amounts of palladium, $Pd(PPh_3)_4$, selectively removes the Alloc group and thus permits the synthesis of the second part of the platform. To ensure competitive yields at each reaction step during the fabrication of the platform, the powerful HATU/DIEA[61] and OxymaPure/DIC[62] coupling systems were used. The final step entails the use of an acidic TFA-based mixture to cleave the platform off the resin and deprotect the amino acid side chains. This reaction needs to be done in the presence of DTT, a reductive agent, to prevent from thiol oxidation (i.e., disulfide bridge formation).[63] The final platform containing the RGD and PHSRN motifs was obtained with good yield and purity. This SPPS method represents thus a robust and straightforward approach to produce peptide-based divalent platforms, and holds a great degree of flexibility to introduce other anchors, spacer units, and bioactive sequences.

Biofunctionalization of Ti and Surface Characterization. The platform and the control peptides were dissolved in PBS at 100 μM and physically adsorbed to Ti overnight. This coating concentration was optimized for RGD-based cell adhesive peptides in previous studies[23,24,64] and validated in our coating system for the platform (see Figure S2 in the Supporting Information). Samples biofunctionalized with the platform were also subjected to ultrasonication in distilled water. This mechanical challenge did not result in a significant loss of cell-binding activity (see Figure S2 in the Supporting Information), thereby indicating that the binding of the molecule to Ti is stable enough under the conditions used in cell adhesion studies. This stability was evidenced in previous investigations with Ti surfaces coated with thiolated RGD-based peptides.[24,44,56,57]

The resulting biofunctionalized surfaces were characterized by means of static contact angle measurements and surface energy calculations (Figure 3), white-light interferometry (Table 1), and X-ray photoelectron spectroscopy (XPS) (Table 2, Figure 4).

The immobilization of the platform and the control peptides onto Ti resulted in a significant decrease in the values of static water contact angle (Figure 3A). This reduction, which indicates an increase in the hydrophilicity of the samples, was statistically comparable for all peptides. In contrast, the contact angle of diiodomethane with the surfaces remained unaltered upon peptide functionalization. Consistent with these observations, a clear increase in the polar component of surface energy of the samples was detected (Figure 3B). Thus, the binding of all peptides increased the polarity of the samples to the same extent. Analysis of the surfaces by white light interferometry revealed

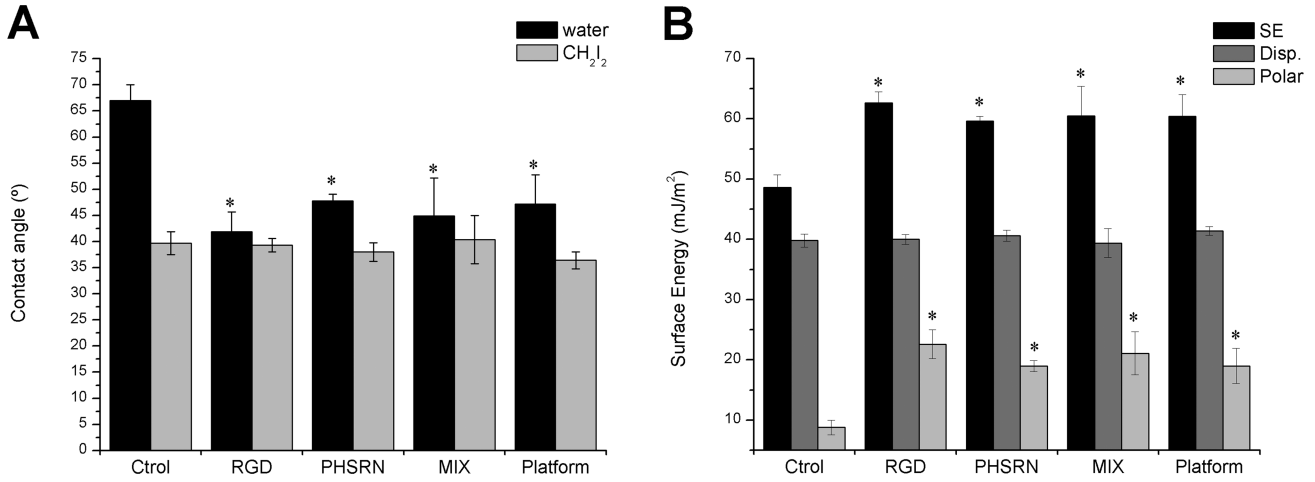

Figure 3. Contact angle measurements and surface energy calculations. (A) Static contact angle values on the biofunctionalized surfaces using water and diiodomethane (CH_2I_2) as wetting liquids (1 μL). (*) $p < 0.05$ vs. Ctrol. (B) Surface energy (SE) values of the biofunctionalized surfaces, and their dispersive (Disp.) and polar components. (*) $p < 0.05$ vs. Ctrol. Values are expressed as mean ± standard deviation.

Table 1. Average Roughness Values (R_a) of the Biofunctionalized Surfaces. Values are Expressed As Mean ± Standard Deviation

	surface				
	Ctrol	RGD	PHSRN	Mix	Platform
R_a (nm)	39.1 ± 6.1	45.0 ± 7.8	42.3 ± 0.9	48.1 ± 16.9	42.7 ± 8.8

Table 2. Analysis of the Chemical Composition (atomic percentages) of the Biofunctionalized Surfaces by XPS. Each Atomic Percentage Is Expressed As Mean ± Standard Deviation

	Composition (atomic %)			
SAMPLE	C 1s	O 1s	N 1s	Ti 2p
Ctrol	23.68 ± 1.12	59.15 ± 1.02	0.67 ± 0.10	16.49 ± 0.21
RGD	24.53 ± 0.93	58.30 ± 0.76	0.99 ± 0.07	16.18 ± 0.34
PHSRN	28.60 ± 0.67	54.19 ± 0.80	2.59 ± 0.11	14.61 ± 0.03
Mix	27.53 ± 1.53	54.60 ± 1.01	2.75 ± 0.14	15.11 ± 0.38
Platform	31.35 ± 0.88	50.92 ± 1.13	4.29 ± 0.63	13.44 ± 0.34

that the roughness of Ti samples was not modified during the process of peptide attachment. Therefore, physisorption, unlike other methods of biomolecule immobilization that require the use of acids or bases to activate the surface,[2,6] did not alter the topography of the surface at the nanometer-level. The wettability, surface energy and topography (i.e., roughness) of biomaterials have been described to have a strong influence in cell adhesion.[42,44,65,66] The fact that all the biofunctionalized surfaces in this study showed comparable values of surface energy and roughness is of relevance, because it indicates that differences in cell behavior on these surfaces may be attributed to the biofunctionality of the molecules deposited onto it and not to other physicochemical properties.

The surfaces were further characterized by XPS analysis, which confirmed changes in the composition and chemistry of Ti samples upon physical adsorption of the platform and control peptides (Table 2). Control Ti samples displayed characteristic signals of C 1s, O 1s, and Ti 2p. The presence of carbon is attributed to atmospheric organic contaminants.[67] A small amount of N contamination was also observed. Functionalization of the samples with peptides yielded an increase in the percentage of C 1s and N 1s and a decrease in that of Ti 2p and O 1s signals. Both effects have been described to be typical indicators of peptide attachment:[31,68,69] in particular, the presence of nitrogen can be attributed to amide groups and other amino functionalities characteristic of peptide sequences, whereas the deposition of a peptide layer reduces the amount of the detectable signal of TiO_2 by XPS. The rate of reduction in the signal of Ti 2p is consistent with the formation of a submonolayer to monolayer of peptide on the surface, which typically shows a thickness below 1 nm.[31,68] In particular, analysis of the attenuation of the Ti 2p3/2 signal after immobilization of the platform revealed a layer thickness of 0.5 nm for this molecule (see the Supporting Information for details). Such layer thickness has been associated with peptide densities in the range of 4−6 pmol/cm^2,[31] which are high enough to support efficient cell adhesion and spreading.[70]

The most remarkable effects were found for the platform, consistent with the higher molecular weight of this molecule. However, the fact that all control samples contained C and N contaminants makes impossible to define precise ratios to quantitatively compare the efficiency of the attachment of the different biomolecules, as can be done for instance when using silicon as internal reference (i.e., study of N/Si ratios).[68,69] Thus, estimations of the extent of biofunctionalization for each surface on this study should be taken with caution.

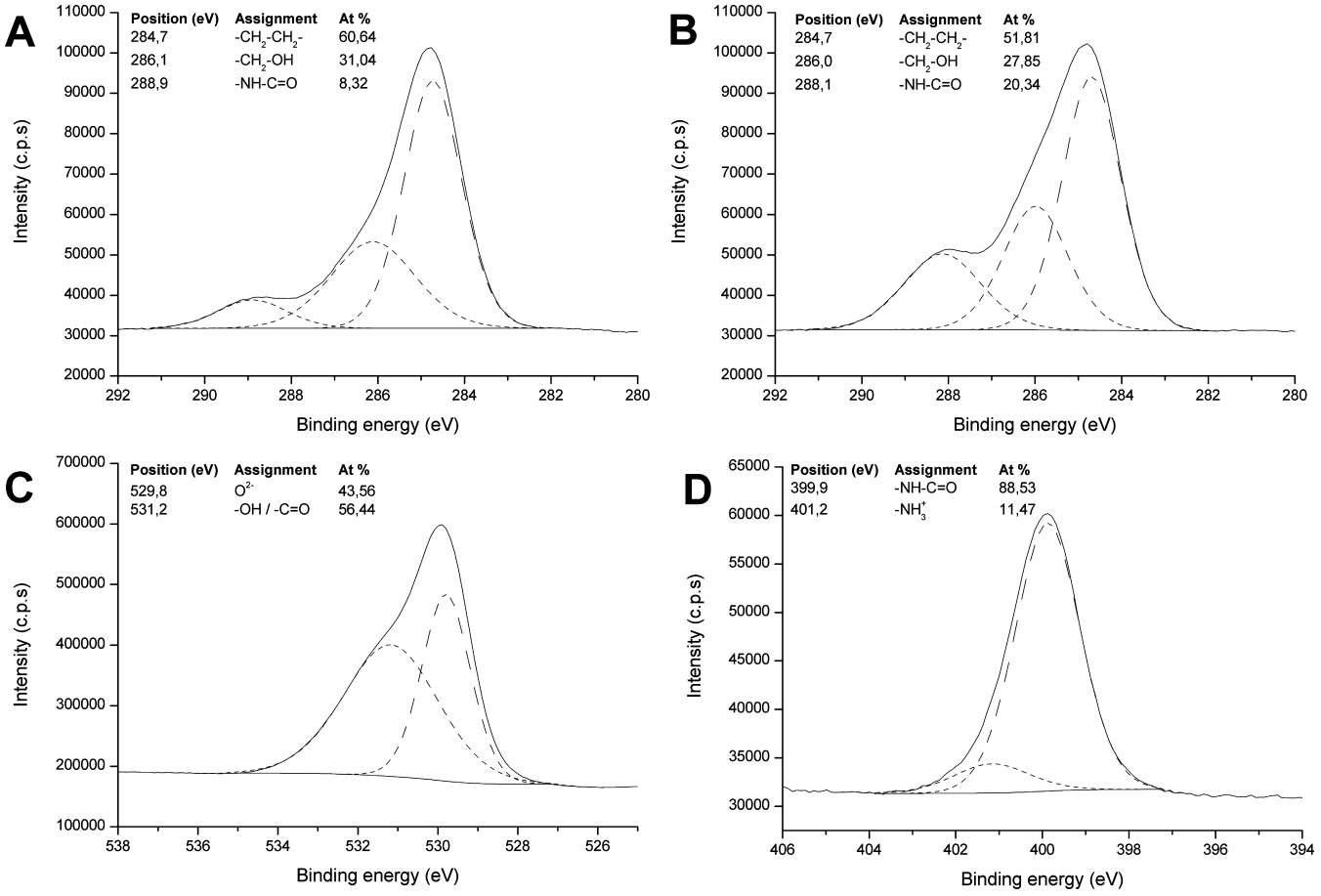

Figure 4. Curve-fitting deconvolutions of high resolution XPS spectra. (A) C 1s spectrum of non-functionalized control surfaces; and (B) C 1s, (C) O 1s and (D) N 1s spectra of surfaces functionalized with the platform. Dashed lines represent the fitting components and solid lines the sum of these components. For each spectrum, the position, assignment and atomic percentage (At %) of the deconvoluted peaks are detailed.

Deconvolution of high-resolution spectra of the samples proved useful to study the process of biofunctionalization. The presence of hydrocarbon contaminants in the C 1s spectra of Ctrol surfaces (Figure 4A) was characterized by a major peak at 284.7 eV assigned to aliphatic carbons ($-CH_2-CH_2-$). Two more peaks were observed at higher binding energies. A peak at 286.1 eV is typical of carbons bound to amines ($-CH_2-NH_2$) or alcohols/alkoxy groups ($-CH_2-OH/-CH_2-OR$), whereas at 288.9 eV it designates more polar carbonyl groups. The attachment of the platform to Ti significantly increased the intensity of this peak (Figure 4B), which was shifted to 288.1 eV. This binding energy is characteristic of amide groups ($-NH-C=O$). The presence of the platform was further confirmed by the analysis of the O 1s and N 1s spectra (Figures 4C and 4D). The O 1s peak has two main contributions at binding energies of 529.8 and 531.2 eV. The first peak is attributed to oxides (O^{2-}) of the Ti surface layer. The second peak can be assigned to carbonyl groups ($-C=O$), especially amides, and probably overlaps with the signal of surface hydroxyl groups (Ti−OH, typically at 531-532 eV). The intensity of this peak is significantly higher compared to Ctrol samples (data not shown). The analysis of the N 1s peak also revealed a major peak at 399.9 eV, which corresponds to amide groups. The other minor peak appears at 401.2, a region of positively charged free amines, and may be due to charged guanidine groups present in arginine (Arg).[68] Because the detection of amide groups can be unequivocally associated with the presence of peptides sequences, the XPS analysis is consistent with a successful attachment of the platform onto Ti. Deconvolutions of the samples biofunctionalized with the control peptides showed similar fittings and are not shown here.

Cell Response on the Biofunctionalized Surfaces. The response of Saos-2 cells to the biofunctionalized surfaces was evaluated in vitro by means of cell adhesion, proliferation and differentiation assays. This cell system has been described as an adequate model to study osseointegration in vitro.[71]

The results of early adhesion events (number of cells attached and their spreading) are shown in Figure 5. After 4 h of incubation, the presence of RGD peptides slightly increased the number of cells attached onto the surfaces compared to Ctrol samples (Figure 5A). As expected, this effect was not observed when the synergy motif PHSRN was presented alone.[33] The combination of RGD and PHSRN sequences, either as a mixture or presented in the platform, also displayed an enhancement in the number of cells adhered in regard to controls, but to the same extent than the RGD peptide. These results indicate that the presence of the synergy sequence on these surfaces did not have a measurable biological effect in terms of cell adhesion capacity for this cell system. It should also be mentioned that statistically significant differences were just observed for the positive control FN, and thus these data may be regarded only as a trend. The simultaneous presentation of the RGD motif and its synergy sequence PHSRN, however, did have a remarkable influence on the spreading behavior of these cells (Figures 5B and 6). The RGD peptide significantly increased the area of the cells

dx.doi.org/10.1021/am5001213 | ACS Appl. Mater. Interfaces 2014, 6, 6525−6536

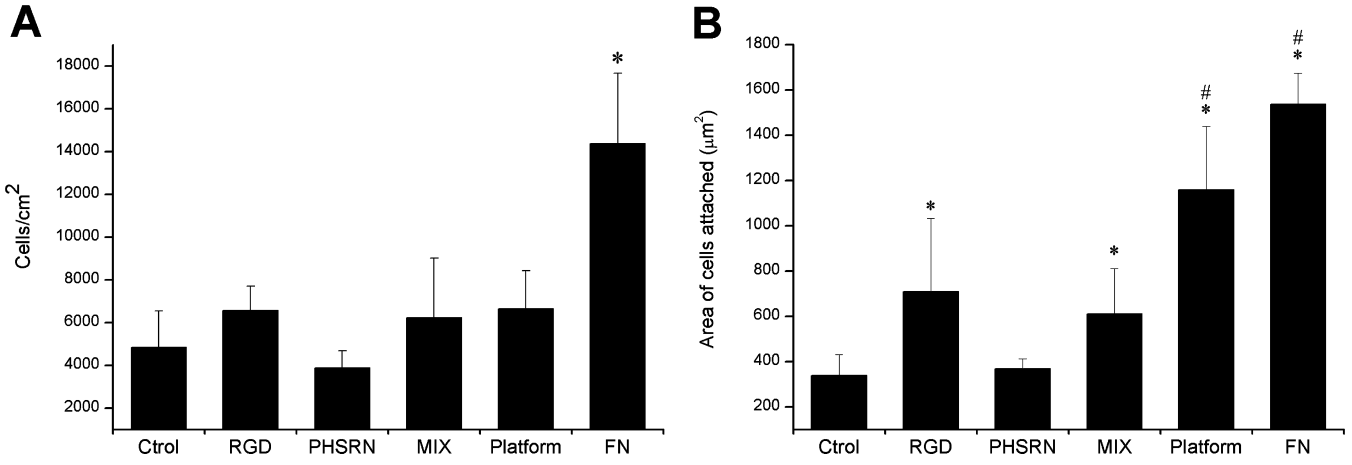

Figure 5. Adhesion of Saos-2 cells on biofunctionalized surfaces after 4h of incubation. (A) Number of cells attached (cells/cm^2) was analyzed by means of an LDH assay. (*) $p < 0.05$ vs. other conditions. (B) Area of cells attached (μm^2) was studied by labeling of actin filaments with phalloidin-rodhamine and fluorescence microscopy. (*) $p < 0.05$ vs. Ctrol and PHSRN; (#) $p < 0.05$ vs. RGD and MIX. Values are expressed as mean ± standard deviation.

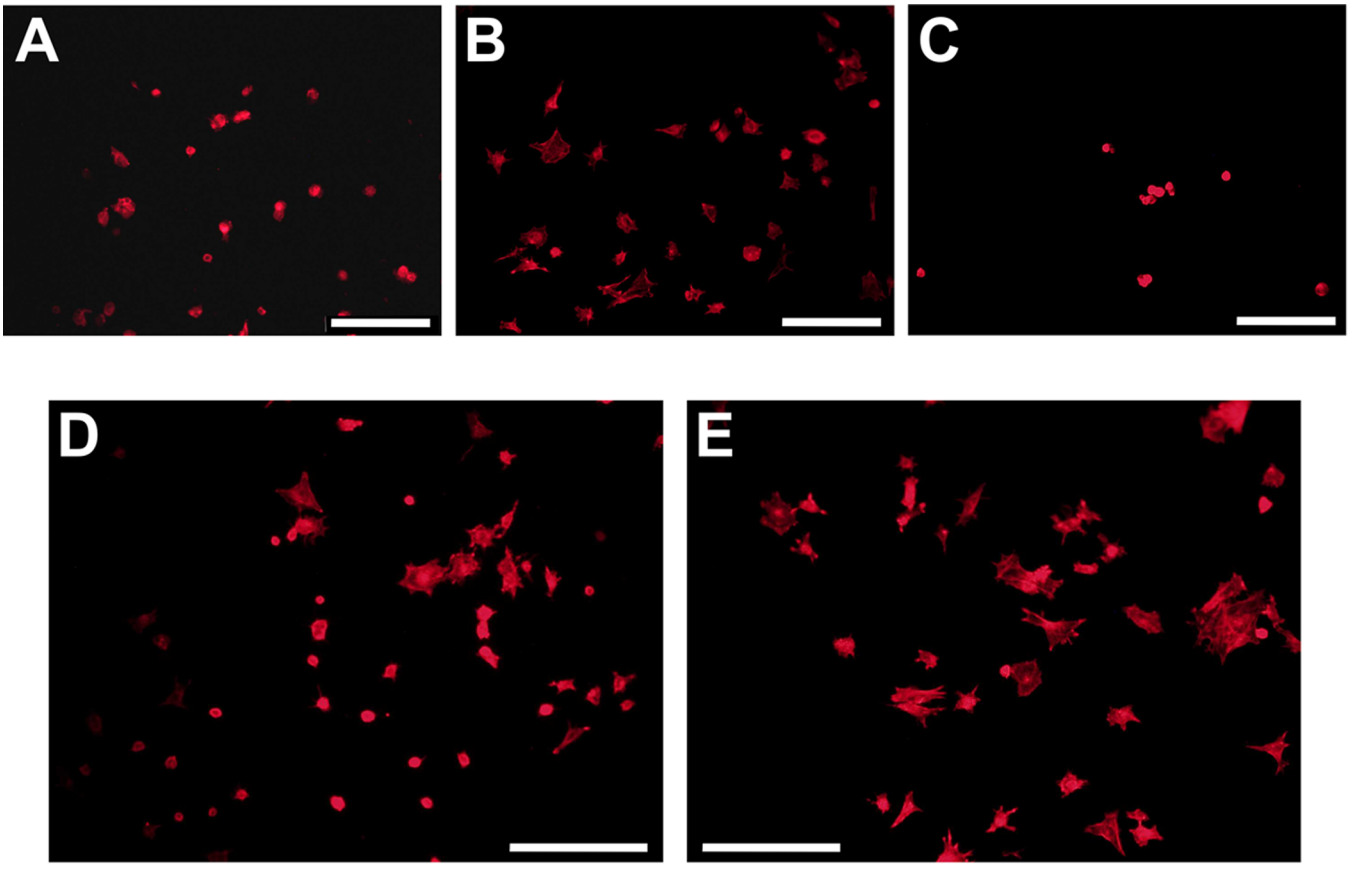

Figure 6. Spreading of Saos-2 cells on biofunctionalized surfaces after 4h of incubation. (A) Ctrol, (B) RGD, (C) PHSRN, (D) MIX, and (E) Platform. Cell spreading on FN-coated samples is shown in the Supporting Information as Figure S3. Images were acquired by fluorescence microscopy and show only staining of actin filaments with phalloidin-rodhamine. Scale bars: 200 μm.

compared to Ctrol and PHSRN-coated samples, where cells were clearly round and not spread. This effect was statistically increased when this peptide was combined with PHSRN in the platform, reaching levels of spreading close to those observed for FN samples (Figure 5B and Figure S3 in the Supporting Information). Such observation is in accordance with previous studies and may be attributed to a higher $\alpha5\beta1$-binding activity of the platform compared to the RGD sequence.[35,39,40,51] Other authors, in contrast, have reported an $\alpha v\beta3$-dependent activity for a molecule containing RGD and PHSRN sequences separated by a 13-Gly spacer.[46] However, the elucidation of the precise role of these integrins in cell adhesion studies is complex and would require further experiments that are beyond the scope of this work. Interestingly, this synergistic effect was not observed when the two motifs were combined as a mixture (Figure 5B). A closer analysis on the spreading behavior of Saos-2 onto surfaces coated with the platform and the mixture revealed further differences (Figure 6). Whereas the platform supported a

dx.doi.org/10.1021/am5001213 | ACS Appl. Mater. Interfaces 2014, 6, 6525−6536

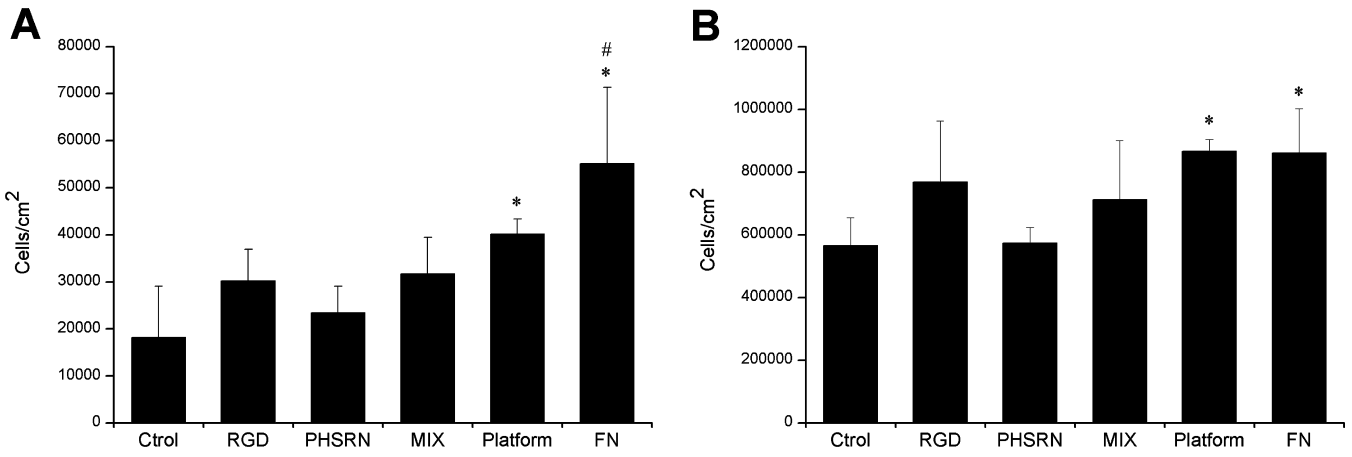

Figure 7. Proliferation of Saos-2 cells on biofunctionalized surfaces. The number of cells was determined by LDH assays. (A) Proliferation after 3 days of incubation. (*) $p < 0.1$ vs. Ctrol, PHSRN and MIX; (#) $p < 0.1$ vs. RGD. (B) Proliferation after 14 days of incubation. (*) $p < 0.1$ vs. Ctrol and PHSRN. Values are expressed as mean ± standard deviation.

very homogeneous spreading all over the surface, with cells displaying defined actin filaments and a clear cytoskeletal organization, the spreading of cells onto the surfaces coated with the mixture was not homogeneous, with some areas presenting cells very well spread, and other areas with cells totally round (Figure 6D, E). We hypothesize that this observation is due to a random orientation and spacing of the RGD and PHSRN binding motifs in the mixture, which in some cases match the optimal distance and spatial conformation for receptor binding, and in others not. On the contrary, the platform presents the two motifs always at the same distance in a chemically defined fashion. Moreover, the branched presentation obtained with this architecture might ensure the correct accessibility of the active motifs for cell-expressed surface receptors. These results are not in agreement with a recent work from Aparicio and coworkers, who showed enhancing effects when combining mixtures of RGD and PHSRN onto Ti surfaces.[37] However, in their work, a different method of peptide immobilization was used, and they were able to show an homogenous co-localization of the two peptide sequences over the surface. The importance of the relative orientation of these two motifs to interact with integrins has already been emphasized,[21,38,45,46] but it represents a critical issue also for other active sequences. For instance, in recent studies the combination of RGD with the heparin-binding sequence KRSR did not result in enhanced biological activities as was expected.[72,73] The authors reasoned that these negative outcomes were due to the fact that the peptides were anchored randomly on the surfaces at distances and positions not defined, which did not show an optimal conformation to interact with the target cells. In another study, the linear presentation of the RGD and KRSR sequences, separated by a short spacer, did not display either increased cell adhesive properties on coated-surfaces. Again, the specific spatial arrangement required for the two peptides to interact with cell receptors was probably not present.[74]

The presence of focal adhesions onto the biofunctionalized samples was also analyzed by immunostaining of vinculin. However, clear focal adhesions could not be detected at this short time point (4 h of incubation) for this cell line. Only some nascent focal points were observed for FN-coated samples and to a lower extent for some RGD- or platform-coated samples (data not shown).

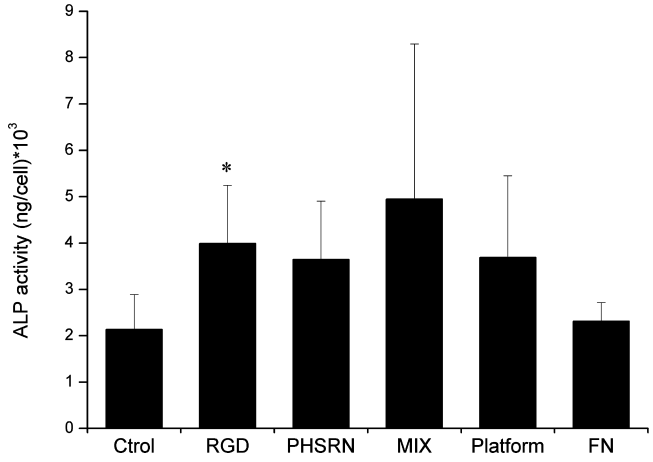

Figure 8. Production of ALP by Saos-2 cells on biofunctionalized surfaces. The production of ALP was measured after 14 days of incubation using a standard colorimetric method. (*) $p < 0.1$ vs. Ctrol and FN. Values are expressed as mean ± standard deviation.

The capacity of adherent cells to proliferate on these surfaces was also analyzed at two different time points (Figure 7). After 3 days of incubation, an increased proliferation rate was observed on Ti surfaces coated with the RGD peptide, the mixture of motifs and the platform, compared to Ctrol samples. Within these treatments, the platform showed the highest values of cell proliferation. Noteworthy, the same trend was maintained after 14 days of culture, with the platform showing values of proliferation comparable to the positive control FN. Saos-2 cells are known to express high levels of ALP, a characteristic osteoblastic phenotype, when cultured onto Ti surfaces.[71] In our study, the presence of the platform on the surfaces supported good levels of ALP production by these cells after 14 days of incubation (Figure 8). However, only RGD-coated samples showed a statistically significant enhanced ALP activity compared to Ctrol samples. Reduced phenotype expression has been associated with high values of initial spreading and cell proliferation,[75] therefore the modest values of ALP expressed on FN samples should not come as a surprise.

The results described here encourage further work. The physical adsorption of molecules onto surfaces is useful to study cell-material interactions, but it may not provide an anchoring to

dx.doi.org/10.1021/am5001213 | ACS Appl. Mater. Interfaces 2014, 6, 6525−6536

Ti as stable as other methods of covalent immobilization. Therefore, other approaches such as silanization should be considered to use this platform for medical applications. In this regard, the platform contains as anchoring group a thiol, whose nucleophilic character allows the reaction with electrophilic centers or with α,β-unsaturated carbonyl molecules (i.e. maleimide groups used as crosslinkers with amino-functionalized silanes). To corroborate that, we conducted a preliminary study binding the platform to Ti via organosilanes (see the experimental procedure and Figure S4 in the Supporting Information). Noteworthy, this strategy significantly improved the adhesion of Saos-2 cells compared to controls. These preliminary data prove silanization as a viable future strategy. Moreover, the interaction of this platform with $\alpha v\beta 3$ and $\alpha 5\beta 1$ integrins and its effect on cell differentiation should be studied with detail. These two approaches are ongoing work in our group.

CONCLUSIONS

In summary, we have described a reliable and flexible synthetic protocol to produce peptide-based divalent platforms with the capability to present two distinct bioactive motifs in a chemically defined and controlled fashion. As a proof of concept, a platform containing the RGD and PHSRN sequences was synthesized and immobilized onto Ti by physical adsorption. The successful attachment of the biomolecule was characterized by XPS analysis. Surfaces coated with the platform efficiently supported and promoted good levels of attachment, spreading, proliferation, and differentiation of osteoblast-like cells. These biological effects were less pronounced when the two motifs were randomly distributed over the surface, stressing the importance of an appropriate accessibility and spatial orientation of the ligands to cell-expressed surface receptors. It has become evident that the combination of functionalities may successfully emulate complex and dynamic biological processes and may dramatically improve the performance of implant materials. Thus, the use of this platform to combine cell adhesive peptides with other biologically relevant sequences opens new prospects for promising applications in the fields of biomaterials and tissue engineering.

ASSOCIATED CONTENT

Supporting Information

HPLC chromatogram of the purified platform, calculation of the thickness of the peptide layer, and supplementary cell adhesion experiments. This material is available free of charge via the Internet at http://pubs.acs.org.

AUTHOR INFORMATION

Corresponding Author

*E-mail: carles.mas.moruno@upc.edu. Tel: (+34) 934010814. Fax: (+34) 934016706.

Author Contributions

The manuscript was written through contributions of all authors. All authors have given approval to the final version of the manuscript.

Notes

The authors declare no competing financial interest.

ACKNOWLEDGMENTS

This study was supported by the Ministry of Economy and Competitiveness (MINECO) of the Spanish Government (Project: MAT2012-30706) and the Agency for Administration of University and Research Grants of the Government of Catalonia (SGR2009 1039). C.M.-M. thanks the support of the Secretary for Universities and Research of the Ministry of Economy and Knowledge of the Government of Catalonia (2011-BP-B-00042) and the People Programme (Marie Curie Actions) of the European Union's Seventh Framework Programme (FP7-PEOPLE-2012-CIG, REA grant agreement 321985). R.F. thanks the Government of Catalonia for a predoctoral fellowship. The authors also express their gratitude to Mrs. Montse Domínguez for her useful technical assistance regarding the XPS analysis.

REFERENCES

(1) Shekaran, A.; Garcia, A. J. Extracellular Matrix-Mimetic Adhesive Biomaterials for Bone Repair. *J. Biomed. Mater. Res., Part A* **2011**, *96*, 261−272.

(2) Bauer, S.; Schmuki, P.; von der Mark, K.; Park, J. Engineering Biocompatible Implant Surfaces Part I: Materials and Surfaces. *Prog. Mater. Sci.* **2013**, *58*, 261−326.

(3) von der Mark, K.; Park, J. Engineering Biocompatible Implant Surfaces Part II: Cellular Recognition of Biomaterial Surfaces: Lessons from Cell-Matrix Interactions. *Prog. Mater. Sci.* **2013**, *58*, 327−381.

(4) Siebers, M. C.; ter Brugge, P. J.; Walboomers, X. F.; Jansen, J. A. Integrins as Linker Proteins between Osteoblasts and Bone Replacing Materials. A Critical Review. *Biomaterials* **2005**, *26*, 137−146.

(5) López-García, M.; Kessler, H. Stimulation of Bone Growth on Implants by Integrin Ligands. In *Handbook of Biomineralization*; Epple, M., Bäuerlein, E., Eds. Wiley-VCH: Weinheim, Germany, 2007; pp 109−126.

(6) Mas-Moruno, C.; Espanol, M.; Montufar, E. B.; Mestres, G.; Aparicio, C.; Gil, F. J.; Ginebra, M. -P. Bioactive Ceramic and Metallic Surfaces for Bone Engineering. In *Biomaterials Surface Science*; Taubert, A., Mano, J. F., Rodríguez-Cabello, J. C., Eds.; Wiley-VCH: Weinheim, Germany, 2013; pp 337−374.

(7) Williams, D. F. The Role of Short Synthetic Adhesion Peptides in Regenerative Medicine; The Debate. *Biomaterials* **2011**, *32*, 4195−4197.

(8) Moursi, A. M.; Globus, R. K.; Damsky, C. H. Interactions between Integrin Receptors and Fibronectin Are Required For Calvarial Osteoblast Differentiation In Vitro. *J. Cell. Sci.* **1997**, *110*, 2187−2196.

(9) Lee, M. H.; Ducheyne, P.; Lynch, L.; Boettiger, D.; Composto, R. J. Effect of Biomaterial Surface Properties on Fibronectin-$\alpha 5\beta 1$ Integrin Interaction and Cellular Attachment. *Biomaterials* **2006**, *27*, 1907−1916.

(10) Geißler, U.; Hempel, U.; Wolf, C.; Scharnweber, D.; Worch, H.; Wenzel, K. W. Collagen Type I-Coating of Ti6Al4V Promotes Adhesion of Osteoblasts. *J. Biomed. Mater. Res.* **2000**, *51*, 752−760.

(11) Rammelt, S.; Schulze, E.; Bernhardt, R.; Hanisch, U.; Scharnweber, D.; Worch, H.; Zwipp, H.; Biewener, A. Coating of Titanium Implants with Type-I Collagen. *J. Orthop. Res.* **2004**, *22*, 1025−1034.

(12) Welander, M.; Abrahamsson, I.; Linder, E.; Liljenberg, B.; Berglundh, T. Soft Tissue Healing at Titanium Implants Coated with Type I Collagen. An Experimental Study in Dogs. *J. Clin. Periodontol.* **2007**, *34*, 452−458.

(13) Petrie, T. A.; Raynor, J. E.; Reyes, C. D.; Burns, K. L.; Collard, D. M.; Garcia, A. J. The Effect of Integrin-Specific Bioactive Coatings on Tissue Healing and Implant Osseointegration. *Biomaterials* **2008**, *29*, 2849−2857.

(14) Petrie, T. A.; Reyes, C. D.; Burns, K. L.; Garcia, A. J. Simple Application of Fibronectin-Mimetic Coating Enhances Osseointegration of Titanium Implants. *J. Cell. Mol. Med.* **2009**, *13*, 2602−2612.

(15) Rico, P.; González-García, C.; Petrie, T. A.; García, A. J.; Salmerón-Sánchez, M. Molecular Assembly and Biological Activity of a Recombinant Fragment of Fibronectin (FNIII7−10) on Poly(ethyl acrylate). *Colloid. Surf., B* **2010**, *78*, 310−316.

(16) Martino, M. M.; Mochizuki, M.; Rothenfluh, D. A.; Rempel, S. A.; Hubbell, J. A.; Barker, T. H. Controlling Integrin Specificity and Stem Cell Differentiation in 2D and 3D Environments through Regulation of Fibronectin Domain Stability. *Biomaterials* **2009**, *30*, 1089−1097.

(17) Collier, J. H.; Segura, T. Evolving the Use of Peptides as Components of Biomaterials. *Biomaterials* **2011**, *32*, 4198−4204.
(18) Bellis, S. L. Advantages of RGD Peptides for Directing Cell Association with Biomaterials. *Biomaterials* **2011**, *32*, 4205−4210.
(19) Pierschbacher, M. D.; Ruoslahti, E. Cell Attachment Activity of Fibronectin Can Be Duplicated by Small Synthetic Fragments of the Molecule. *Nature* **1984**, *309*, 30−33.
(20) Hersel, U.; Dahmen, C.; Kessler, H. RGD Modified Polymers: Biomaterials for Stimulated Cell Adhesion and Beyond. *Biomaterials* **2003**, *24*, 4385−4415.
(21) Barker, T. H. The Role of ECM Proteins and Protein Fragments in Guiding Cell Behavior in Regenerative Medicine. *Biomaterials* **2011**, *32*, 4211−4214.
(22) Heckmann, D.; Kessler, H. Design and Chemical Synthesis of Integrin Ligands. *Methods Enzymol.* **2007**, *426*, 463−503.
(23) Kantlehner, M.; Schaffner, P.; Finsinger, D.; Meyer, J.; Jonczyk, A.; Diefenbach, B.; Nies, B.; Hölzemann, G.; Goodman, S. L.; Kessler, H. Surface Coating with Cyclic RGD Peptides Stimulates Osteoblast Adhesion and Proliferation as Well as Bone Formation. *ChemBioChem.* **2000**, *1*, 107−114.
(24) Dahmen, C.; Auernheimer, J.; Meyer, A.; Enderle, A.; Goodman, S. L.; Kessler, H. Improving Implant Materials by Coating with Nonpeptidic, Highly Specific Integrin Ligands. *Angew. Chem., Int. Ed.* **2004**, *43*, 6649−6652.
(25) Rechenmacher, F.; Neubauer, S.; Polleux, J.; Mas-Moruno, C.; De Simone, M.; Cavalcanti-Adam, E. A.; Spatz, J. P.; Fässler, R.; Kessler, H. Functionalizing $\alpha v\beta 3$- or $\alpha 5\beta 1$-Selective Integrin Antagonists for Surface Coating: A Method to Discriminate Integrin Subtypes In Vitro. *Angew. Chem., Int. Ed.* **2013**, *52*, 1572−1575.
(26) Rechenmacher, F.; Neubauer, S.; Mas-Moruno, C.; Dorfner, P. M.; Polleux, J.; Guasch, J.; et al. A Molecular Toolkit to Functionalize Ti-Based Biomaterials that Selectively Control Integrin-Mediated Cell Adhesion. *Chem. - Eur. J.* **2013**, *19*, 9218−9223.
(27) Rahmouni, S.; Lindner, A.; Rechenmacher, F.; Neubauer, S.; Sobahi, T. R.; Kessler, H.; Cavalcanti-Adam, E. A.; Spatz, J. P. Hydrogel Micropillars with Integrin Selective Peptidomimetic Functionalized Nanopatterned Tops: A New Tool for the Measurement of Cell Traction Forces Transmitted through $\alpha v\beta 3$- or $\alpha 5\beta 1$-Integrins. *Adv. Mater.* **2013**, *25*, 5869−5874.
(28) Dee, K. C.; Andersen, T. T.; Bizios, R. Design and Function of Novel Osteoblast-Adhesive Peptides for Chemical Modification of Biomaterials. *J. Biomed. Mater. Res.* **1998**, *40*, 371−377.
(29) Hasenbein, M. E.; Andersen, T. T.; Bizios, R. Micropatterned Surfaces Modified with Select Peptides Promote Exclusive Interactions with Osteoblasts. *Biomaterials* **2002**, *23*, 3937−3942.
(30) Rezania, A.; Healy, K. E. Biomimetic Peptide Surfaces that Regulate Adhesion, Spreading, Cytoskeletal Organization, and Mineralization of the Matrix Deposited by Osteoblast-Like Cells. *Biotechnol. Prog.* **1999**, *15*, 19−32.
(31) Rezania, A.; Johnson, R.; Lefkow, A. R.; Healy, K. E. Bioactivation of Metal Oxide Surfaces. 1. Surface Characterization and Cell Response. *Langmuir* **1999**, *15*, 6931−6939.
(32) Schuler, M.; Hamilton, D. W.; Kunzler, T. P.; Sprecher, C. M.; de Wild, M.; Brunette, D. M.; Textor, M.; Tosatti, S. G. Comparison of the Response of Cultured Osteoblasts and Osteoblasts Outgrown from Rat Calvarial Bone Chips to Nonfouling KRSR and FHRRIKA-Peptide Modified Rough Titanium Surfaces. *J. Biomed. Mater. Res., Part B* **2009**, *91*, 517−527.
(33) Aota, S.; Nomizu, M.; Yamada, K. M. The Short Amino Acid Sequence Pro-His-Ser-Arg-Asn in Human Fibronectin Enhances Cell-Adhesive Function. *J. Biol. Chem.* **1994**, *269*, 24756−24761.
(34) Dillow, A. K.; Ochsenhirt, S. E.; McCarthy, J. B.; Fields, G. B.; Tirrell, M. Adhesion of $\alpha 5\beta 1$ Receptors to Biomimetic Substrates Constructed from Peptide Amphiphiles. *Biomaterials* **2001**, *22*, 1493−1505.
(35) Mardilovich, A.; Craig, J. A.; McCammon, M. Q.; Garg, A.; Kokkoli, E. Design of a Novel Fibronectin-Mimetic Peptide-Amphiphile for Functionalized Biomaterials. *Langmuir* **2006**, *22*, 3259−3264.
(36) Ochsenhirt, S. E.; Kokkoli, E.; McCarthy, J. B.; Tirrell, M. Effect of RGD Secondary Structure and the Synergy Site PHSRN on Cell Adhesion, Spreading and Specific Integrin Engagement. *Biomaterials* **2006**, *27*, 3863−3874.
(37) Chen, X.; Sevilla, P.; Aparicio, C. Surface Biofunctionalization by Covalent Co-Immobilization of Oligopeptides. *Colloid. Surf., B* **2013**, *107*, 189−197.
(38) Kao, W. J.; Lee, D.; Schense, J. C.; Hubbell, J. A. Fibronectin Modulates Macrophage Adhesion and FBGC Formation: The Role of RGD, PHSRN, and PRRARV Domains. *J. Biomed. Mater. Res.* **2001**, *55*, 79−88.
(39) Kim, T. I.; Jang, J. H.; Lee, Y. M.; Ryu, I. C.; Chung, C. P.; Han, S. B.; Choi, S. M.; Ku, Y. Design and Biological Activity of Synthetic Oligopeptides with Pro-His-Ser-Arg-Asn (PHSRN) and Arg-Gly-Asp (RGD) Motifs for Human Osteoblast-Like Cell (MG-63) Adhesion. *Biotechnol. Lett.* **2002**, *24*, 2029−2033.
(40) Benoit, D. S. W.; Anseth, K. S. The Effect on Osteoblast Function of Colocalized RGD and PHSRN Epitopes on PEG Surfaces. *Biomaterials* **2005**, *26*, 5209−5220.
(41) Susuki, Y.; Hojo, K.; Okazaki, I.; Kamata, H.; Sasaki, M.; Maeda, M.; Nomizu, M.; Yamamoto, Y.; Nakagawa, S.; Mayumi, T.; et al. Preparation and Biological Activities of a Bivalent Poly(ethylene glycol) Hybrid Containing an Active Site and its Synergistic Site of Fibronectin. *Chem. Pharm. Bull.* **2002**, *50*, 1229−1232.
(42) Pegueroles, M.; Aparicio, C.; Bosio, M.; Engel, E.; Gil, F. J.; Planell, J. A.; Altankov, G. Spatial Organization of Osteoblast Fibronectin Matrix on Titanium Surfaces: Effects of Roughness, Chemical Heterogeneity and Surface Energy. *Acta Biomater.* **2010**, *6*, 291−301.
(43) Pegueroles, M.; Tonda-Turo, C.; Planell, J. A.; Gil, F.-J.; Aparicio, C. Adsorption of Fibronectin, Fibrinogen, and Albumin on TiO2: Time-Resolved Kinetics, Structural Changes, and Competition Study. *Biointerphases* **2012**, *7*, 48.
(44) Mas-Moruno, C.; Dorfner, P. M.; Manzenrieder, F.; Neubauer, S.; Reuning, U.; Burgkart, R.; Kessler, H. Behavior of Primary Human Osteoblasts on Trimmed and Sandblasted Ti6Al4V Surfaces Functionalized with Integrin $\alpha v\beta 3$-Selective Cyclic RGD Peptides. *J. Biomed. Mater. Res., Part A* **2013**, *101*, 87−97.
(45) Grant, R. P.; Spitzfaden, C.; Altroff, H.; Campbell, I. D.; Mardon, H. J. Structural Requirements for Biological Activity of the Ninth and Tenth FIII Domains of Human Fibronectin. *J. Biol. Chem.* **1997**, *272*, 6159−6166.
(46) Petrie, T. A.; Capadona, J. R.; Reyes, C. D.; Garcia, A. J. Integrin Specificity and Enhanced Cellular Activities Associated with Surfaces Presenting a Recombinant Fibronectin Fragment Compared to RGD Supports. *Biomaterials* **2006**, *27*, 5459−5470.
(47) Leahy, D. J.; Aukhil, I.; Erickson, H. P. 2.0 Å Crystal Structure of a Four-Domain Segment of Human Fibronectin Encompassing the RGD Loop and Synergy Region. *Cell* **1996**, *84*, 155−164.
(48) Johansson, S.; Svineng, G.; Wennerberg, K.; Armulik, A.; Lohikangas, L. Fibronectin-Integrin Interactions. *Front. Sci. Ser.* **1997**, *2*, d126−146.
(49) Kao, W. J.; Lee, D. In Vivo Modulation of Host Response and Macrophage Behavior by Polymer Networks Grafted with Fibronectin-Derived Biomimetic Oligopeptides: The Role of RGD and PHSRN Domains. *Biomaterials* **2001**, *22*, 2901−2909.
(50) Schmidt, D. R.; Kao, W. J. Monocyte Activation in Response to Polyethylene Glycol Hydrogels Grafted with RGD and PHSRN Separated by Interpositional Spacers of Various Lengths. *J. Biomed. Mater. Res., Part A* **2007**, *83*, 617−625.
(51) Ahmed, S.; Yang, H. K.; Ozcam, A. E.; Efimenko, K.; Weiger, M. C.; Genzer, J.; Haugh, J. M. Poly(vinylmethylsiloxane) Elastomer Networks as Functional Materials for Cell Adhesion and Migration Studies. *Biomacromolecules* **2011**, *12*, 1265−1271.
(52) Pallarola, D.; Bochen, A.; Boehm, H.; Rechenmacher, F.; Sobahi, T. R.; Spatz, J. P.; Kessler, H. Interface Immobilization Chemistry of cRGD-based Peptides Regulates Integrin Mediated Cell Adhesion. *Adv. Funct. Mater.* **2014**, *24*, 943−956.

(53) Love, J. C.; Estroff, L. A.; Kriebel, J. K.; Nuzzo, R. G.; Whitesides, G. M. Self-Assembled Monolayers of Thiolates on Metals as a Form of Nanotechnology. *Chem. Rev.* **2005**, *105*, 1103−1169.
(54) Langel, W.; Menken, L. Simulation of the Interface between Titanium Oxide and Amino Acids in Solution by First Principles MD. *Surf. Sci.* **2003**, *538*, 1−9.
(55) Song, D.-P.; Chen, M.-J.; Liang, Y.-C.; Bai, Q.-S.; Chen, J.-X.; Zheng, X.-F. Adsorption of Tripeptide RGD on Rutile TiO2 Nanotopography Surface in Aqueous Solution. *Acta Biomater.* **2010**, *6*, 684−694.
(56) Elmengaard, B.; Bechtold, J. E.; Soballe, K. In Vivo Study of the Effect of RGD Treatment on Bone Ongrowth on Press-Fit Titanium Alloy Implants. *Biomaterials* **2005**, *26*, 3521−3526.
(57) Elmengaard, B.; Bechtold, J. E.; Soballe, K. In Vivo Effects of RGD-Coated Titanium Implants Inserted in Two Bone-Gap Models. *J. Biomed. Mater. Res., Part A* **2005**, *75*, 249−255.
(58) Auernheimer, J.; Zukowski, D.; Dahmen, C.; Kantlehner, M.; Enderle, A.; Goodman, S. L.; Kessler, H. Titanium Implant Materials with Improved Biocompatibility via Coating with Cyclic RGD-Peptides via Phosphonates. *ChemBioChem.* **2005**, *6*, 2034−2040.
(59) Mas-Moruno, C.; Cascales, L.; Mora, P.; Cruz, L. J.; Pérez-Payá, E.; Albericio, F. Design and Facile Solid-Phase Synthesis of Peptide-Based LPS Inhibitors Containing PEG-Like Functionalities. *Biopolymers* **2009**, *92*, 508−517.
(60) Farrera-Sinfreu, J.; Royo, M.; Albericio, F. Undesired Removal of the Fmoc Group by the Free ε-Amino Function of a Lysine Residue. *Tetrahedron Lett.* **2002**, *43*, 7813−7815.
(61) Carpino, L. A. 1-Hydroxy-7-azabenzotriazole. An Efficient Peptide Coupling Additive. *J. Am. Chem. Soc.* **1993**, *115*, 4397−4398.
(62) Subirós-Funosas, R.; Prohens, R.; Barbas, R.; El-Faham, A.; Albericio, F. Oxyma: An Efficient Additive for Peptide Synthesis to Replace the Benzotriazole-Based HOBt and HOAt with a Lower Risk of Explosion. *Chem.—Eur. J.* **2009**, *15*, 9394−9403.
(63) Mora, P.; Mas-Moruno, C.; Tamborero, S.; Cruz, L. J.; Pérez-Payá, E.; Albericio, F. Design of a Minimized Cyclic Tetrapeptide that Neutralizes Bacterial Endotoxins. *J. Pept. Sci.* **2006**, *12*, 491−496.
(64) Jeschke, B.; Meyer, J.; Jonczyk, A.; Kessler, H.; Adamietz, P.; Meenen, N. M.; Kantlehner, M.; Goepfert, C.; Nies, B. RGD-Peptides for Tissue Engineering of Articular Cartilage. *Biomaterials* **2002**, *23*, 3455−3463.
(65) Kennedy, S. B.; Washburn, N. R.; Simon, C. G., Jr; Amis, E. J. Combinatorial Screen of the Effect of Surface Energy on Fibronectin-Mediated Osteoblast Adhesion, Spreading and Proliferation. *Biomaterials* **2006**, *27*, 3817−3824.
(66) Guillem-Marti, J.; Delgado, L.; Godoy-Gallardo, M.; Pegueroles, M.; Herrero, M.; Gil, F. J. Fibroblast Adhesion and Activation onto Micro-Machined Titanium Surfaces. *Clin. Oral Impl. Res.* **2013**, *24*, 770−780.
(67) Healy, K. E.; Ducheyne, P. J. Oxidation Kinetics of Titanium Thin Films in Model Physiologic Environments. *J. Colloid Interface Sci.* **1992**, *150*, 404−417.
(68) Xiao, S. J.; Textor, M.; Spencer, N. D.; Wieland, M.; Keller, B.; Sigrist, H. Immobilization of the Cell-Adhesive Peptide Arg−Gly−Asp−Cys (RGDC) on Titanium Surfaces by Covalent Chemical Attachment. *J. Mater. Sci.: Mater. Med.* **1997**, *8*, 867−872.
(69) Xiao, S. J.; Textor, M.; Spencer, N. D.; Sigrist, H. Covalent Attachment of Cell-Adhesive, (Arg-Gly-Asp)-Containing Peptides to Titanium Surfaces. *Langmuir* **1998**, *14*, 5507−5516.
(70) Massia, S. P.; Hubbell, J. A. An RGD Spacing of 440 nm Is Sufficient for Integrin αvβ3-Mediated Fibroblast Spreading and 140 nm for Focal Contact and Stress Fiber Formation. *J. Cell Biol.* **1991**, *114*, 1089−1100.
(71) Shapira, L.; Halabi, A. Behavior of Two Osteoblast-Like Cell Lines Cultured on Machined or Rough Titanium Surfaces. *Clin. Oral Implants Res.* **2009**, *20*, 50−55.
(72) Bell, B. F.; Schuler, M.; Tosatti, S.; Textor, M.; Schwartz, Z.; Boyan, B. D. Osteoblast Response to Titanium Surfaces Functionalized with Extracellular Matrix Peptide Biomimetics. *Clin. Oral Impl. Res.* **2011**, *22*, 865−872.
(73) Broggini, N.; Tosatti, S.; Ferguson, S. J.; Schuler, M.; Textor, M.; Bornstein, M. M.; Bosshardt, D. D.; Buser, D. Evaluation of Chemically Modified SLA Implants (modSLA) Biofunctionalized with Integrin (RGD)- and Heparin (KRSR)-Binding Peptides. *J. Biomed. Mater. Res., Part A* **2012**, *100*, 703−711.
(74) Dettin, M.; Conconi, M. T.; Gambaretto, R.; Pasquato, A.; Folin, M.; Di Bello, C.; Parnigotto, P. P. Novel Osteoblast-Adhesive Peptides for Dental/Orthopedic Biomaterials. *J. Biomed. Mater. Res.* **2002**, *60*, 466−471.
(75) Tosatti, S.; Schwartz, Z.; Campbell, C.; Cochran, D. L.; VandeVondele, S.; Hubbell, J. A.; Denzer, J. A.; Simpson, J.; Wieland, M.; Lohmann, C. H.; et al. RGD-Containing Peptide GCRGYGRGDSPG Reduces Enhancement of Osteoblast Differentiation by Poly(L-lysine)-graft-poly(ethylene glycol)-Coated Titanium Surfaces. *J. Biomed. Mater. Res., Part A* **2004**, *68*, 458−472.